Cancer Management and Research

Dovepress

open access to scientific and medical research

Open Access Full Text Article

ORIGINAL RESEARCH

Long Non-Coding RNA XIST Promotes Wilms Tumor Progression Through the miR-194-5p/YAP Axis

This article was published in the following Dove Press journal:
Cancer Management and Research

Xingyue He[1]
Xin Luo[2]
Junjun Dong[1]
Xing Deng[1]
Feng Liu[1,2]
Guanghui Wei[1,2]

[1]Department of Urology, Children's Hospital of Chongqing Medical University, National Clinical Research Center for Child Health and Disorders, Ministry of Education Key Laboratory of Child Development and Disorders, Chongqing, People's Republic of China; [2]Chongqing Key Laboratory of Children Urogenital Development and Tissue Engineering; Chongqing Key Laboratory of Pediatrics, Chongqing, People's Republic of China

Purpose: Although the long non-coding RNA (lncRNA) X inactive-specific transcript (XIST) has been reported to have an anti-tumor effect in multiple malignant tumors, its role in Wilms tumor (WT) progression has not been characterized. Thus, we investigated the underlying mechanism by which XIST regulates WT progression.

Patients and Methods: We performed microarray analysis and real-time quantitative PCR (RT-qPCR) to detect the expression levels of XIST lncRNA, microRNA-194-5p (miR-194-5p), and YAP (yes-associated protein in Hippo pathway) in tumor and matched adjacent normal tissues and blood collected from 49 WT patients. We also conducted bioinformatics analyses to identify differentially expressed genes. We measured the effects of XIST overexpression and knockdown on cell proliferation, apoptosis, migration, and invasion, and its association with the miR-194-5p/YAP pathway in the rhabdoid G401cell line using flow cytometry, transwell assays, immunohistochemistry, Western blot analysis, and the dual luciferase reporter gene assay.

Results: We found that XIST lncRNA levels were increased in blood and tissue samples of WT patients, and this upregulation was significantly correlated with TNM staging and shorter survival time. Notably, we found that XIST upregulation correlated with miR-194-5p downregulation and YAP upregulation in WT tissues, suggesting that XIST regulates the miR-194-5p/YAP pathway. Conversely, XIST downregulation inhibited WT cell proliferation, migration, and invasion and induced apoptosis. Our study revealed the oncogenic role of the lncRNA XIST in WT and demonstrated its role as a competitive endogenous RNA that regulates the miR-194-5p/YAP pathway.

Conclusion: Our study demonstrates XIST's potential as a clinical prognostic biomarker and therapeutic target for WT.

Keywords: lncRNA, XIST, Wilms tumor, YAP

Introduction

As the most common malignant solid tumor among children 2–3 years of age, Wilms tumor (WT) is a representative treatment model for malignant childhood kidney cancer.[1] Although tumors are generally fatal, more than 85% of patients with tumors confined to the primary tumor site can be completely cured.[2] However, over the past 10 years, the prognosis of WT patients in the high-risk group with unresectable tumors, primary metastasis, and high recurrence, has been poor.[3,4] The National WT Study 5 (NWTS-5) group concluded that the loss of heterozygosity on chromosomes 1p and 16q is a high-risk factor for WT recurrence and death, but it is

Correspondence: Feng Liu; Guanghui Wei
Department of Urology, Children's Hospital of Chongqing Medical University, National Clinical Research Center for Child Health and Disorders, Ministry of Education Key Laboratory of Child Development and Disorders, 136, Zhongshan 2nd Road, Yuzhong District, Chongqing, 400014, People's Republic of China
Tel +8613983693965; +8613883617398
Email liuu_ff@163.com; u806806@cqmu.edu.cn

submit your manuscript | www.dovepress.com
DovePress
http://doi.org/10.2147/CMAR.S297842

not associated with tumor stage and histological type.[5] With more WT genetic research focused on gaining a deeper understanding of WT etiology, identifying effective therapeutic targets and reliable biomarkers of WT could improve tumor prognosis.

Long non-coding RNA (lncRNA) was originally thought to be transcriptional "noise" and a by-product of RNA polymerase II transcription and had no biological functions.[6] It was later discovered that lncRNA can regulate vital processes such as X chromosome silencing, transcription activation, transcription interference, nuclear transport, and a variety of pathological processes during tumorigenesis, progression, and metastasis. LncRNA single nucleotide polymorphisms (SNPs) have been implicated in WT pathogenesis, and previous studies have attempted to uncover the relationship between polymorphisms in the lncRNA LINC00673 and WT susceptibility.[7,8] The anti-tumor role of the lncRNA XIST (X inactive-specific transcript) was found from observations of its aberrant expression in malignant tumors, including colorectal cancer,[9] liver cancer,[10] and gastric cancer.[11] As XIST's role in WT has not been characterized, we designed this study to determine if XIST plays a role in WT tumor progression.

MicroRNA (miRNAs) are another group of non-coding RNAs that contain between 20–25 nucleotides. MiRNAs can target gene expression through translation inhibition or mRNA cleavage, as well as participate in cell proliferation, differentiation, and apoptosis. Aberrant miRNA expression can lead to carcinogenesis or tumor suppression.[12,13] Although miR-194-5p has been reported to inhibit metastasis and epithelial-mesenchymal transition in WT,[14] its association with XIST in WT remains to be verified.

The evolutionarily conserved Hippo/yes-associated protein (YAP) signaling pathway, which was originally discovered in Drosophila, plays a key role in tissue homeostasis and regulating organ size. The core protein YAP in the pathway is aberrantly expressed in pediatric tumors rhabdomyosarcoma, Ewing's sarcoma, osteosarcoma, neuroblastoma, and liver cancer.[15] Notably, genome-wide analysis in podocytes revealed associations between the Hippo/YAP pathway and the transcription factor WT suppressor 1 (WT1). WT1 germline mutations were discovered to be common in adolescents with WT.[16] As the role of YAP in WT has not been clarified, we sought to measure its expression level in WT, as well as its correlation with XIST lncRNA.

Materials and Methods

Patient Information and Sample Collection

WT tissue (tumor group) and adjacent normal renal tissue (normal group) of 49 patients aged 4–11 years old who underwent WT surgery in the Department of Urology, Children's Hospital of Chongqing Medical University, China, were collected between September 2017 and January 2020. Blood samples from 2 WT patients and 2 healthy children were also collected. After resection, the tumor tissue and adjacent kidney tissue were frozen in liquid nitrogen. All specimens were diagnosed as WT by two independent pathologists and were graded according to the NWTS-5 classification and TNM staging system. None of the patients received radiotherapy or chemotherapy before surgery. The correlation between clinicopathological characteristics and the expression of target lncRNA was analyzed using the collected patient clinical data. This study was carried out in accordance with the World Medical Association Declaration of Helsinki and approved by the Ethics Committee of the Children's Hospital of Chongqing Medical University, China. Written informed consent was obtained from all parents of patients.

Blood lncRNA/mRNA Chromatin Immunoprecipitation (ChIP)-Sequencing

Total RNA was extracted from blood samples from 2 WT and 2 healthy children using Trizol reagent (Invitrogen, Carlsbad, CA, USA) according to the manufacturer's instructions, followed by purification using the NucleoSpin® RNA clean-up kit (MACHEREY-NAGEL, Germany). RNA purity and concentration were determined using a spectrophotometer (NanoDrop ND-1000) based on the OD260/280 readings, and RNA integrity was assessed using 1% formaldehyde denaturing gel electrophoresis. ChIP was next performed using the human lncRNA array v4 lab-on-a-chip kit (CapitalBio Technology, Beijing, China) according to the manufacturer's instructions, and the results were analyzed using the GeneSpring software V13.0 (Agilent). Differentially expressed genes were identified using the following cutoff criteria: fold-change > 2 and $P \leq 0.05$. Hierarchical clustering was performed for data classification (Cluster 3.0 software) prior to bioinformatics analyses.

Reverse Transcription-Quantitative PCR (RT-qPCR)

Total RNA from WT and adjacent normal tissues was extracted using Trizol reagent and the concentration was measured using a UV spectrophotometer. Reverse

transcription to cDNA was performed using the PrimeScript™ RT kit (Qiagen) according to the manufacturer's instructions. RT-qPCR (SYBR Premix Ex Taq™, TAKARA) was performed using primers with the following sequences: XIST, F: 5′-AA CCACCACACGTCAAGCTCTTC-3′, R: 5ÁGTGC CAGGCATGTTGATCTTCAG-3′; miR-194-5p, F: 5′-cgTGTAACAGCAACTCCATGTGGA-3′; YAP: F: 5′-TAGCCCTGCGTAGCCAGTTA-3′, R: 5′-TCATGCT TAGTCCACTGTCTGT-3′. The following RT-qPCR reaction conditions were used: Cycle: 95°C for 30 s, 95°C for 5 s, and 60°C for 45 s, repeated for 40 cycles. Quantification of lncRNA and miRNA in tissues was calculated using the $2^{-\Delta\Delta CT}$ method. Three experimental replicates of each sample were obtained and the average was calculated.

Lentiviral Transfection

LncRNA XIST overexpression (XIST), XIST sh-RNA knockdown (sh-XIST), and empty control lentiviral vectors (negative control NC and sh-NC, respectively) (GenechemCo, Ltd., Shanghai, China) were transduced into 293T cells. The XIST overexpression sequence was based on the fragment XIST:13 (https://lncipedia.org/). The packaged lentiviral vectors were then transfected into the human WT G401 rhabdoid cell line (ATCC, USA) according to the manufacturer's protocol and were collected for analysis after 48 h. The miR-194-5p mimic and NC mimic plasmids (GenePharma, Shanghai, China) were transfected into the human WT G401 cell line using Lipofectamine™ RNAiMAX (Invitrogen, USA) according to the manufacturer's protocol.

Cell Lines and Cell Culture

Human WT G401 and normal renal tubular epithelial HK-2 cell lines (ATCC, USA) were cultured in DMEM medium containing 10% fetal bovine serum (FBS) and 1% penicillin/streptomycin (Gibco, USA) at 37°C, in a 5% CO_2 humidified incubator.

Western Blot Analysis

Total protein was extracted from tissues and transfected cell lines using RIPA lysis buffer (Beyotime, China) supplemented with 1% phenylmethanesulfonyl fluoride (PMSF). Protein concentration was determined using the BCA assay. The proteins were separated using SDS-PAGE and transferred onto a polyvinylidene fluoride (PVDF) membrane. The membrane was first incubated with a YAP rabbit primary antibody (1:1,000; cat. #14074, CST, USA) at 4°C overnight followed by a goat anti-rabbit HRP-conjugated secondary antibody (WLA023; Wanleibio, China). The bands were detected and visualized using an enhanced chemiluminescence kit (Millipore, USA) and Quantity One software (Bio-Rad, USA) was used for image acquisition and density analysis.

Immunohistochemistry

Tissue specimens from patients who did not receive WT preoperative treatment were fixed with 4% neutral buffered formalin for 6–72 h within 30 min after isolation. Eight pairs of tumor tissues and adjacent normal tissues were then randomly selected for immunohistochemistry. The formalin-fixed specimens were next subjected to paraffin embedding, sectioning (4 μm-thick, 2 mm diameter), dewaxing, rehydration, and antigen retrieval. Next, the sections were incubated in 3% hydrogen peroxide and 0.5% bovine serum albumin (BSA) for 25 min prior to the addition of rabbit anti-YAP primary antibody (1:100 dilution; CST, USA), which was incubated overnight at 4°C. The sections were subsequently incubated with HRP-conjugated goat anti-rabbit IgG secondary antibody (1:500 dilution; Jackson Immuno Research, USA) for 50 min at 37°C, and were finally stained with 100 μL 3,3′-diaminobenzidine (DAB) and hematoxylin (ZSGB-BIO, China) for visualization under an inverted microscope (Nikon, Japan).

Cell Proliferation and Apoptosis Detection

The CCK-8 (cell counting kit) cell viability assay was used to detect the effect of XIST and sh-XIST lentiviral transfection on the proliferation of G401 cells according to the manufacturer's protocol (Biosharp, China). Briefly, G401 cells (5×10^3/well) after lentiviral transfection were seeded in 96-well plates at 37°C and were divided into 4 groups (0, 1, 2, and 3 days) of 5 wells/group. After 25 h, the cells were incubated with CCK-8 solution (10 μL) for 2 h at 37°C before cell viability assessment. Absorbance at wavelength 450 nm was measured using a microplate reader (Bio-Rad, USA). Triplicate measurements were obtained.

Transfected G401 cells were subjected to Annexin V-FITC/propidium iodide (PI) staining (kit purchased from KeyGEN, China) to assess cell apoptosis. Briefly, cells were incubated with Annexin V-FITC/PI staining solution for 15 min in the dark according to the

manufacturer's protocol before flow cytometry (BD Biosciences, USA) and analysis using the FlowJo software to determine the apoptotic rate. Three independent experiments were performed.

Cell Migration and Invasion

Wound healing assays were used to evaluate cell migration. G401 cells (1×10^5/well) transfected with XIST and sh-XIST lentivirus were seeded in a 6-well plate. When cell confluence reached 90%, a straight line (scratch) was drawn in the middle of the plate using a 10 μL pipette tip. Cells that did not adhere to the plate were washed away with phosphate buffered saline (PBS) and replaced with fresh cell culture medium without FBS. At 0, 24, and 48 h, images of the cells were captured and analyzed using the ImageJ software.

The transwell assay was used to assess cell invasion following G401 cell lentiviral transfection. Briefly, 200 μL of transfected G401 cells (1×10^5/mL) were seeded on the top transwell chamber (50 μL of Matrigel at 1:7 dilution; BD, USA), and 600 μL of complete medium was added to the bottom chamber. After 24 h, the cells were fixed with 90% ethanol and stained with 0.5% crystal violet prior to observation under an inverted microscope (Nikon, Japan). Five fields of view were randomly selected for counting the stained cells.

Dual Luciferase Gene Reporter Assay

GV272 plasmids containing the firefly luciferase gene and wild-type (wt; GV272-XIST-wt and GV272-YAP-wt) or mutant (mut; GV272-XIST-mut and GV272-YAP-mut) fragments of the XIST 3-untranslated region (UTR) with the predicted miR-194-5p binding site (GenechemCo, Ltd. Shanghai, China) were transfected into 293T cells. Briefly, 1 μg plasmid and 2 μL X-tremegene HP transfection reagent (Roche) in 100 μL opti-MEM medium were added to the 293T cells inoculated in a 24-well plate. The cells were cultured at 37°C for 5–6 h in a 5% CO_2 humidified incubator. Complete medium containing 10% serum (200 μL) was added to each well for a total volume of 500 μL. A GFP (green fluorescence protein) plasmid was used as a transfection control. Cells were harvested 48 h after transfection, and luciferase activity was measured using the Dual-Luciferase® Reporter Assay System (Promega, Madison, WI, USA). The firefly luciferase activity of each sample was normalized to Renilla luciferase activity.

Statistical Analysis

Statistical data analysis was performed using the GraphPad Prism software (GraphPad Software Inc, La Jolla, CA, USA) and SPSS v17.0 software (SPSS Inc., Chicago, IL, USA). All data are expressed as the mean ± standard deviation (SD). One-way analysis of variance (ANOVA) or two-tailed Student's *t*-test was used to compare groups. Values of $P < 0.05$ were considered statistically significant.

Results

XIST Upregulation is Correlated with Poor WT Prognosis

LncRNA ChIP sequencing of blood samples of 2 WT and 2 healthy children revealed 32 upregulated lncRNAs (Supplementary Figure 1A and B). XIST lncRNA was among the 32 upregulated lncRNAs, with a log fold-change value of 4.67 (Figure 1A). We selected the top 10 upregulated and top 10 downregulated lncRNAs identified from ChIP sequencing for RT-qPCR validation using 49 pairs of matched WT and adjacent non-tumor tissue samples. RT-qPCR revealed that ENST00000446912.2, AL157834.2, AK027145.1, and LINC01168 were significantly downregulated in WT tissues, while XIST was upregulated in 19 (39%) WT tissues and downregulated in 30 (61%) WT tissues (Figure 1B and Supplementary Figure 1C–G). Analysis of the relationship between XIST expression and clinicopathological characteristics of WT patients revealed that XIST expression significantly correlated with TNM staging and stage III/IV WT (Table 1). In addition, Kaplan-Meier analysis showed that XIST upregulation was associated with shorter survival time of WT patients (Figure 1C).

YAP is Highly Expressed in Human WT Tissues

We conducted microarray analysis of 2 WT and 2 healthy control samples to identify differentially expressed mRNA targets (Figure 1D). On average, our RT-qPCR results demonstrated an upregulation of YAP mRNA in most WT tissues but not in normal tissues (Figure 1E). Consistent with the RT-qPCR results, Western blot analysis and immunohistochemistry verified the upregulation of YAP protein between 8 randomly selected pairs of WT tissues and adjacent non-tumor tissues (Figure 1G and H).

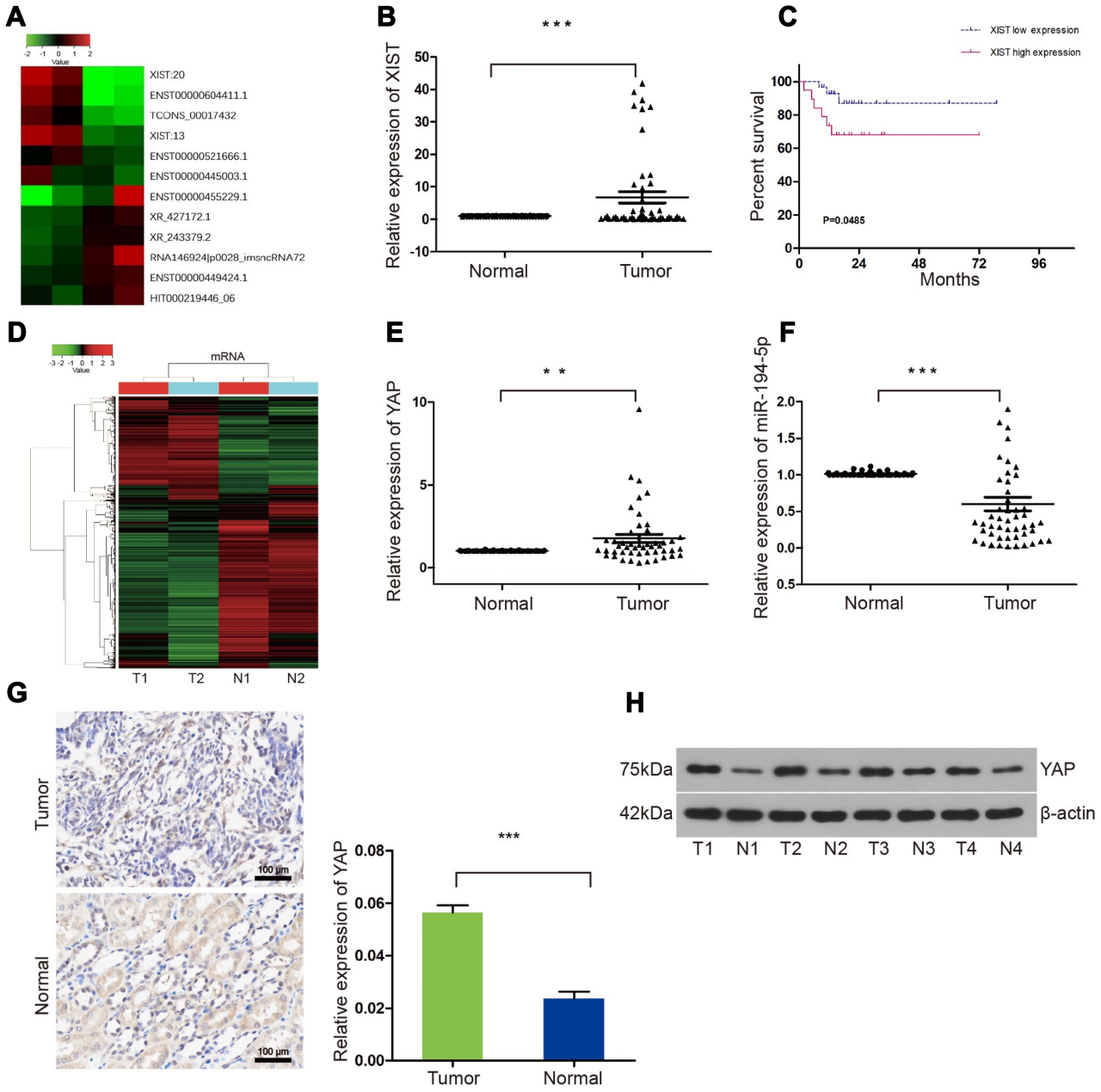

Figure 1 XIST lncRNA, YAP mRNA and protein expression in WT blood and tissue samples. (**A**) ChIP microarray showing differentially expressed lncRNAs in 2 WT and 2 healthy control blood samples. (**B**) RT-qPCR analysis of 49 pairs of matched WT and adjacent non-tumor samples showing the relative expression levels of XIST. (**C**) Kaplan-Meier survival curve of WT patients with differential XIST levels. (**D**) Microarray profiles of differentially expressed mRNA in blood samples of 2 WT patients. (**E** and **F**) RT-qPCR analysis of the relative expression of YAP mRNA and miR-194-5p in WT tissues and adjacent non-tumor tissues (n = 49 each for tumor vs normal tissue). (**G**) Immunohistochemical (400×magnification) and (**H**) Western blot analyses of YAP protein expression levels in 8 randomly selected pairs of WT tissues and adjacent non-tumor tissues. One-way ANOVA or two-tailed *t*-test was performed for comparisons between the two groups. $^{**}P < 0.01$, $^{***}P < 0.001$.
Abbreviations: T, tumor tissue; N, normal tissue.

miR-194-5p Interacts with Both XIST lncRNA and YAP

Using Starbase (http://starbase.sysu.edu.cn/index.php) and TargetScan (http://www.targetscan.org/vert_72/) gene target and binding site prediction programs, we identified miR-194-5p as a target that can bind both XIST lncRNA and YAP and also predicted the miR-194-5p binding site on XIST (Figure 2A) and YAP (Figure 2D). Lower luciferase signal intensity was observed in 293T cells co-transfected with the

Table 1 Relationship Between XIST Expression and the Clinicopathological Features of WT Patients

Characteristics	n	Expression of LncRNA XIST		*P* value
		High Expression	Low Expression	
Sex				
Male	26	12	14	0.260
Female	23	7	16	
Ages				
<3year	28	13	15	0.204
≥3year	21	6	15	
Location				
Left	26	7	19	0.070
Right	23	12	11	
Histological type				
FH	34	12	22	0.451
uFH	15	7	8	
TNM stage				
I, II	32	7	25	0.001*
III, IV, V	17	12	5	
Perinephric metastasis				
Yes	22	9	13	0.782
No	27	10	17	
Lymphatic metastasis				
Yes	12	5	7	0.813
No	37	14	23	
Hematuresis				
Yes	11	4	7	0.852
No	38	15	23	
Tumor size (cm)				
<5	7	2	5	0.239
>5	42	17	15	

Note: *$P < 0.05$.

miR-194-5p mimic and XIST-wt ($P < 0.05$; Figure 2B and C), as well as the miR-194-5p mimic and YAP-wt ($P < 0.05$; Figure 2E and F), compared with the negative control, while no significant change in luciferase activity was observed in the cells co-transfected with the miR-194-5p mimic and either the XIST-mut or YAP-mut. These results suggest that miR-194-5p can bind to both XIST and YAP. Consistent with the observed upregulation of XIST lncRNA and YAP levels (Figure 1B, E, G and H), significant downregulation of miR-194-5p was observed in the tumor tissues of the 49 WT patients (Figure 1F).

XIST lncRNA Regulates WT Through the miR-194-5p/YAP Axis

Consistent with the results from the luciferase reporter assay, RT-qPCR showed that XIST was upregulated (Figure 2G) but miR-194-5p was downregulated (Figure 2H) in G401 WT cells compared with HK-2 normal renal tubular epithelial cells. Moreover, we found that XIST overexpression in the G401 cell line resulted in decreased miR-194-5p levels, while XIST knockdown (sh-XIST) resulted in elevated miR-194-5p levels (Figure 2I). Western blot analysis also verified that YAP protein levels decreased in WT cells upon transfection of miR-194-5p mimic or sh-XIST in G401 WT cells (Figure 2J). Taken together, the results indicate that XIST regulates WT via the miR-194-5p/YAP axis, wherein XIST-mediated repression of miR-194-5p relieves miR-194-5p-mediated inhibition of YAP.

XIST lncRNA Promotes the Proliferation and Invasion of WT Cells

XIST overexpression (XIST; Figure 3A) and knockdown (sh-XIST; Figure 3B) in G401 cells were successfully established. Next, we investigated the effect of XIST lncRNA on G401 WT cells. Using the CCK-8 cell viability assay, we found that XIST enhanced G401 cell proliferation, while sh-XIST attenuated proliferation (Figure 3C and D). Consistent with the results of the CCK-8 assay, flow cytometry analysis showed that XIST decreased WT apoptosis, while sh-XIST promoted WT apoptosis (Figure 3E). Wound healing and transwell assays revealed that overexpression of XIST in G401 cells enhanced WT cell migration and invasion, while sh-XIST suppression decreased cell migration and invasion (Figure 3F and G). These results indicate that XIST promotes the proliferation, migration, and invasion of G401 cells and inhibits apoptosis in vitro, supporting XIST's oncogenic role in WT.

Discussion

There is growing evidence that lncRNA dysregulation can lead to tumorigenesis.[17] The XIST lncRNA is a product of the XIST gene, which plays a primary role in mediating X chromosome inactivation and ensuring

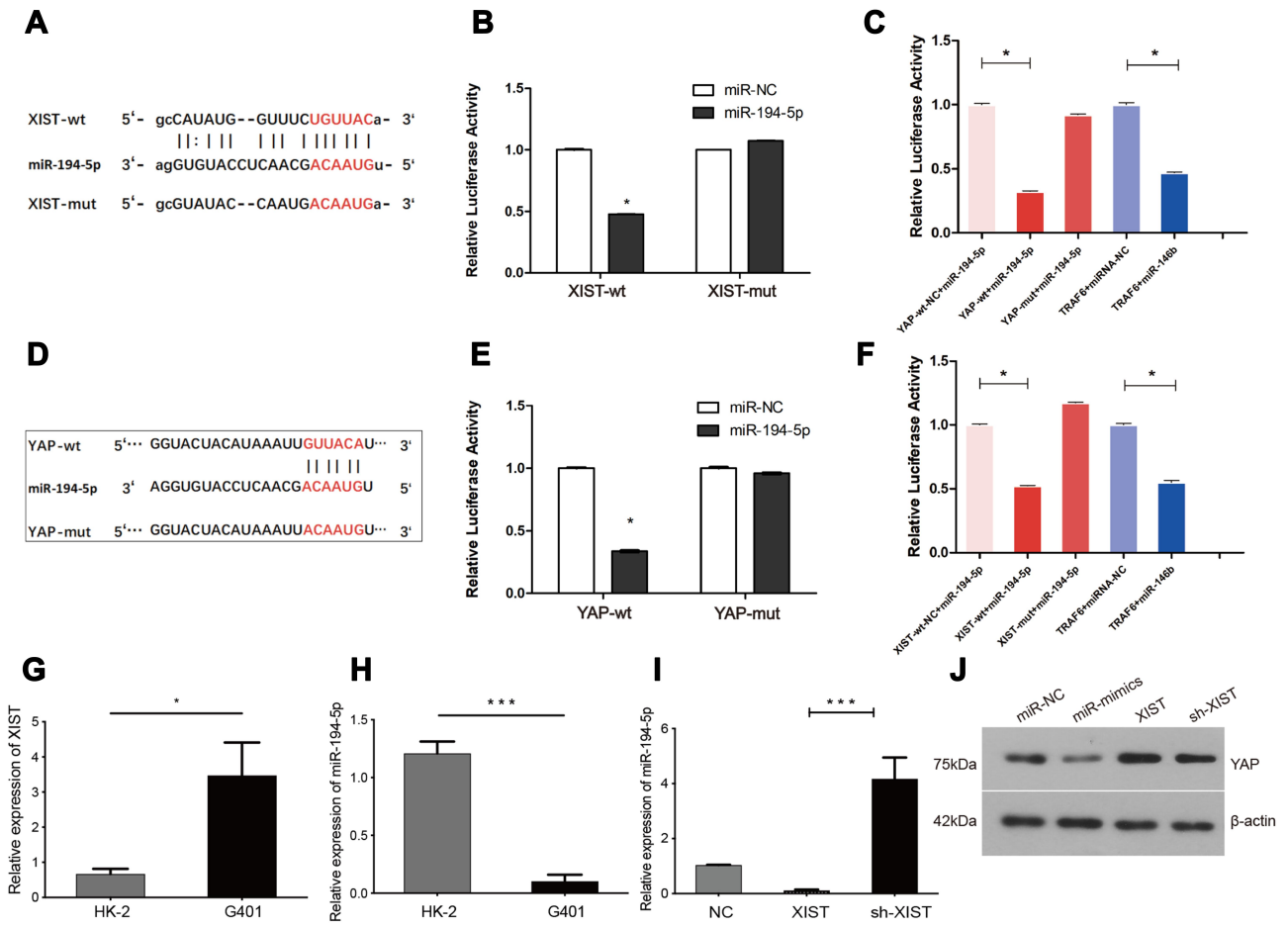

Figure 2 miR-194-5p can bind to both XIST and YAP in WT tissues. XIST lncRNA regulates WT progression through the miR-194-5p/YAP axis. (**A**) XIST 3′-UTR wild-type (XIST-wt) sequence containing the miR-194-5p binding site and sequence of the mutant (XIST-mut) miR-194-5p binding site. (**B** and **C**) Luciferase reporter gene assay (images and histograms) showed lower luciferase activity for miR-194-5p and XIST-wt than XIST-mut ($P < 0.05$). TRAF6 was used as an internal control to verify the integrity of the luciferase gene reporter assay. (**D**) YAP 3′-UTR wild-type (YAP-wt) sequence containing the miR-194-5p binding site and sequence of the mutant (YAP-mut) miR-194-5p binding site. (**E** and **F**) Luciferase reporter gene assay (images and histograms) showed lower luciferase activity for miR-194-5p and YAP-wt than YAP-mut ($P < 0.05$). TRAF6 was used as an internal control to verify the integrity of the luciferase gene reporter assay. (**G**) XIST lncRNA expression and (**H**) miR-194-5p in WT G401 cells and normal renal epithelial HK2 cells. (**I**) RT-qPCR analysis of miR-194-5p after transfection of lentiviral XIST, NC, and sh-XIST in WT G401 cells. (**J**) Western blot analysis showed that YAP protein expression can be regulated by miR-194-5p and XIST. One-way ANOVA or two-tailed *t*-test was performed for comparisons between the two groups. *$P < 0.05$, ***$P < 0.001$.

balanced gene dosage. Notably, XIST upregulation has been observed in some malignant tumors and was found to be associated with tumor cell growth, infiltration, and migration, higher TNM staging, and positive lymph node metastasis.[18] XIST has been shown to function as a "molecular sponge" of miR-139-5p in melanoma,[19] regulate the miR-133a/SOX4 axis in glioma[20] and miR-497 in gastric cancer,[11] and promote cell proliferation, invasion, and metastasis. In addition, XIST methylation status has been reported to modulate prostate cancer progression.[21,22] Since lncRNA has been implicated in WT,[23] we designed this study to elucidate the underlying mechanism of XIST-mediated WT progression. We found elevated XIST levels in WT tissues compared with adjacent non-tumor healthy tissues and also observed a positive correlation between XIST expression levels and survival duration. Bioinformatics prediction and dual luciferase gene reporter assays confirmed that miR-194-5p interacts with both XIST and YAP. Using XIST overexpression and knockdown lentiviral genetic constructs and the G401 WT cell line, we showed that sh-XIST-induced downregulation suppressed cell proliferation, migration, and invasion, and induced apoptosis, while the XIST overexpression constructs reversed these effects. Moreover, our investigation of the underlying mechanism of XIST in WT revealed that XIST lncRNA and YAP protein were upregulated, while miR-194-5p was downregulated in WT. Insights garnered from this study could potentially be applied in WT clinical prognosis and therapy.

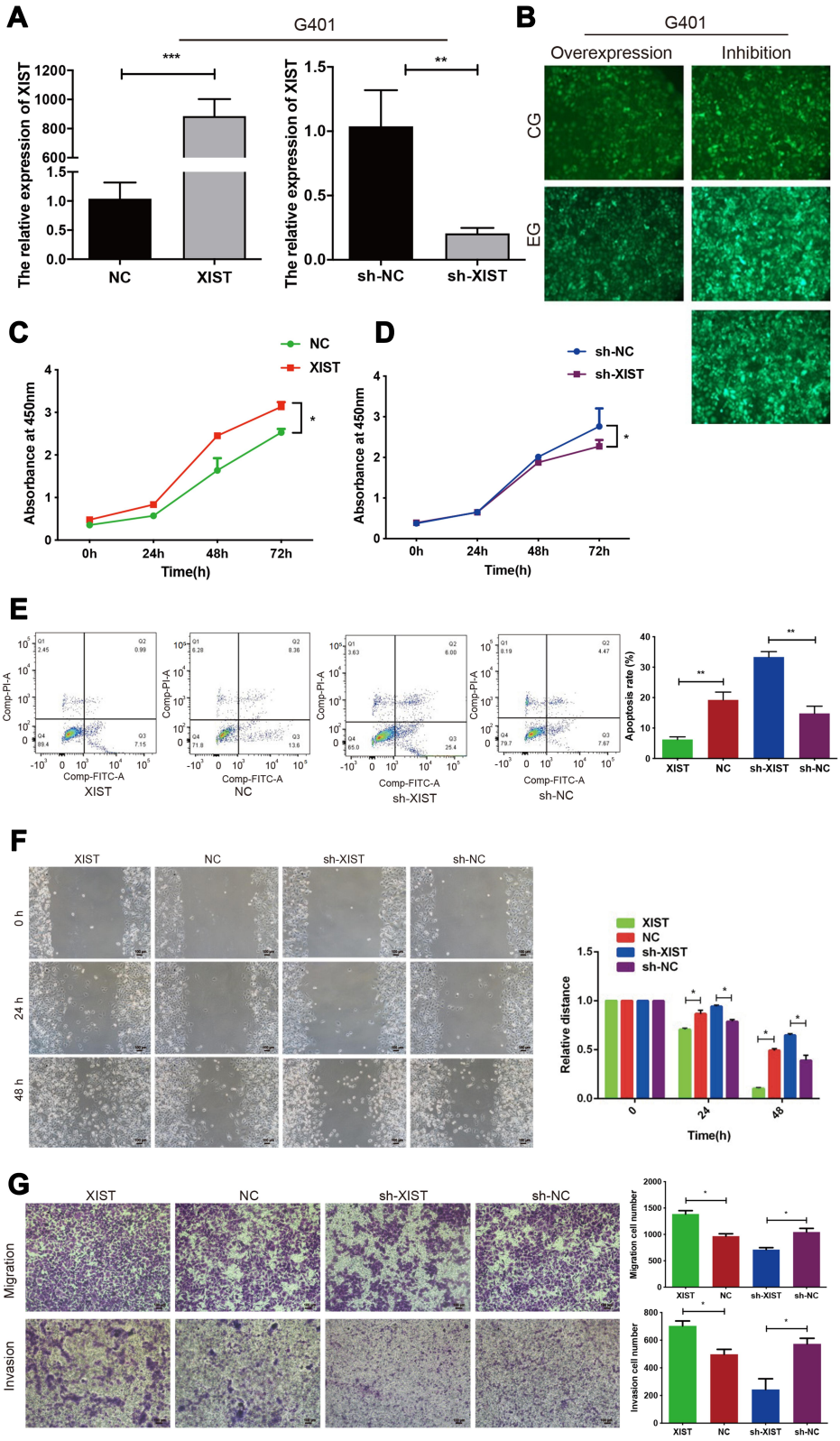

Figure 3 XIST promotes the proliferation, migration, and invasion of G401 cells, and inhibits apoptosis in vitro. (**A** and **B**) Stable XIST overexpression (lentiviral XIST and negative control, NC) and XIST knockdown (lentiviral sh-RNA and negative control, sh-NC) were successfully established in WT G401 cells. (**C**) CCK-8 cell viability assay profiles showed that XIST overexpression enhanced G401 cell proliferation, while (**D**) XIST knockdown decreased cell proliferation. (**E**) Flow cytometry showed that XIST overexpression decreased apoptosis while XIST knockdown promoted apoptosis. (**F**) Scratch assay (100×magnification) (**G**) and transwell assay showed that XIST overexpression promoted G401 cell migration and invasion in vitro (100×magnification). Three independent replicates were performed. One-way ANOVA or two-tailed *t*-test was performed for comparisons between the two groups. **P* < 0.05, ***P* < 0.01, ****P* < 0.001.

In this study, we verified that miR-194-5p was significantly reduced in WT tissues, consistent with a previous report of miR-194-5p-mediated inhibition of metastasis and epithelial-mesenchymal transition in WT, thereby limiting WT progression.[14] After confirming the direct interaction between miR-194-5p, XIST lncRNA, and YAP using the dual luciferase reporter assay, we further verified that miR-194-5p was inhibited by XIST in WT in vivo and in vitro, confirming our hypothesis that XIST plays a role as a competing endogenous RNA (ceRNA) and regulates WT survival. This is the first study to demonstrated that YAP expression is elevated in WT and that XIST lncRNA can modulate YAP protein levels. YAP and miR-194-5p have been reported to be inversely correlated, wherein the former is downregulated and the latter is upregulated upon CG200745 intervention in cholangiocarcinoma cells.[24] We confirmed the association between YAP and miR-194-5p in this study and demonstrated the inhibitory effect of miR-194-5p on downstream YAP expression.

Conclusion

In conclusion, our study revealed the negative correlation between XIST lncRNA expression and WT survival, and we showed that the underlying mechanism of XIST-mediated modulation of WT prognosis involves the miR-194-5p/YAP Hippo signaling pathway. Notably, we are the first group to characterize the association between XIST lncRNA and YAP and their expression in WT. Our findings provide novel insights into improving WT prognosis and therapy.

Data Sharing Statement

The sequencing data can be accessed on the GEO database (GSE166606). Data generated in the current study are available from the corresponding authors Feng Liu and Guanghui Wei upon reasonable request.

Ethics Approval and Consent to Participate

This study was conducted with approval from the Ethics Committee of the Research Institution of Children's Hospital of Chongqing Medical University, and this study was conducted in accordance with the Declaration of Helsinki. The written informed consent was obtained from all parents of patients.

Author Contributions

All authors made substantial contributions to the conception and design, data acquisition, analysis and interpretation, and drafting and editing the manuscript; agreed to submit to the current journal; gave final approval of the version to be published; and agree to be accountable for all aspects of the work.

Funding

This research was supported by the general project of clinical medicine research of Children's Hospital of Chongqing Medical University (NCRC-2019-GP-08).

Disclosure

The authors report no conflicts of interest in this work.

References

1. Lopes RI, Lorenzo A. Recent advances in the management of Wilms' tumor. *F1000Res*. 2017;6:670. doi:10.12688/f1000research.10760.1
2. Bhatnagar S. Management of Wilms' tumor: NWTS vs SIOP. *J Indian Assoc Pediatr Surg*. 2009;14(1):6–14. doi:10.4103/0971-9261.54811
3. Brok J, Lopez-Yurda M, Tinteren HV, et al. Relapse of Wilms' tumour and detection methods: a retrospective analysis of the 2001 Renal Tumour Study Group-International Society of Paediatric Oncology Wilms' tumour protocol database. *Lancet Oncol*. 2018;19(8):1072–1081. doi:10.1016/S1470-2045(18)30293-6
4. Martínez CH, Dave S, Izawa J. Wilms' tumor. *Adv Exp Med Biol*. 2010;685:196–209.
5. Grundy PE, Breslow NE, Li S, et al. Loss of heterozygosity for chromosomes 1p and 16q is an adverse prognostic factor in favorable-histology Wilms tumor: a report from the National Wilms Tumor Study Group. *J Clin Oncol*. 2005;23(29):7312–7321. doi:10.1200/JCO.2005.01.2799
6. Ponting CP, Oliver PL, Reik W. Evolution and functions of long noncoding RNAs. *Cell*. 2009;136(4):629–641. doi:10.1016/j.cell.2009.02.006
7. Li S, Lin A, Han D, et al. LINC00673 rs11655237 C>T and susceptibility to Wilms tumor: a five-center case-control study. *J Gene Med*. 2019;21(12):e3133. doi:10.1002/jgm.3133
8. Zhuo Z, Fu W, Liu J, et al. LIN28A gene polymorphisms confer Wilms tumour susceptibility: a four-centre case-control study. *J Cell Mol Med*. 2019;23(10):7105–7110. doi:10.1111/jcmm.14561
9. Wang KC, Chang HY. Molecular mechanisms of long noncoding RNAs. *Mol Cell*. 2011;43(6):904–914. doi:10.1016/j.molcel.2011.08.018
10. Chang S, Chen B, Wang X, Wu K, Sun Y. Long non-coding RNA XIST regulates PTEN expression by sponging miR-181a and promotes hepatocellular carcinoma progression. *BMC Cancer*. 2017;17(1):248. doi:10.1186/s12885-017-3216-6
11. Ma L, Zhou Y, Luo X, Gao H, Deng X, Jiang Y. Long non-coding RNA XIST promotes cell growth and invasion through regulating miR-497/MACC1 axis in gastric cancer. *Oncotarget*. 2017;8(3):4125–4135. doi:10.18632/oncotarget.13670
12. Salmena L, Poliseno L, Tay Y, Kats L, Pandolfi PP. A ceRNA hypothesis: the Rosetta Stone of a hidden RNA language? *Cell*. 2011;146(3):353–358. doi:10.1016/j.cell.2011.07.014
13. Zhang P, Li J, Song Y, Wang X. MiR-129-5p inhibits proliferation and invasion of chondrosarcoma cells by regulating SOX4/Wnt/β-catenin signaling pathway. *Cell Physiol Biochem*. 2017;42(1):242–253. doi:10.1159/000477323

14. Liu H, Ren SY, Qu Y, et al. MiR-194-5p inhibited metastasis and EMT of nephroblastoma cells through targeting Crk. *Kaohsiung J Med Sci*. 2020;36(4):265–273. doi:10.1002/kjm2.12180
15. Ahmed AA, Mohamed AD, Gener M, Li W, Taboada E. YAP and the Hippo pathway in pediatric cancer. *Mol Cell Oncol*. 2017;4(3): e1295127. doi:10.1080/23723556.2017.1295127
16. Kann M, Ettou S, Jung YL, et al. Genome-wide analysis of Wilms' tumor 1-controlled gene expression in podocytes reveals key regulatory mechanisms. *J Am Soc Nephrol*. 2015;26(9):2097–2104. doi:10.1681/ASN.2014090940
17. Bhan A, Soleimani M, Mandal SS. Long noncoding RNA and cancer: a new paradigm. *Cancer Res*. 2017;77(15):3965–3981. doi:10.1158/0008-5472.CAN-16-2634
18. Yin S, Dou J, Yang G, Chen F. Long non-coding RNA XIST expression as a prognostic factor in human cancers: a meta-analysis. *Int J Biol Markers*. 2019;34(4):327–333. doi:10.1177/1724600819873010
19. Tian K, Sun D, Chen M, et al. Long noncoding RNA X-inactive specific transcript facilitates cellular functions in melanoma via miR-139-5p/ROCK1 pathway. *Onco Targets Ther*. 2020;13:(1277–1287. doi:10.2147/OTT.S225661
20. Luo C, Quan Z, Zhong B, et al. lncRNA XIST promotes glioma proliferation and metastasis through miR-133a/SOX4. *Exp Ther Med*. 2020;19(3):1641–1648. doi:10.3892/etm.2020.8426
21. Martens-Uzunova ES, Böttcher R, Croce CM, Jenster G, Visakorpi T, Calin GA. Long noncoding RNA in prostate, bladder, and kidney cancer. *Eur Urol*. 2014;65(6):1140–1151. doi:10.1016/j.eururo.2013.12.003
22. Song MA, Park JH, Jeong KS, Park DS, Kang MS, Lee S. Quantification of CpG methylation at the 5′-region of XIST by pyrosequencing from human serum. *Electrophoresis*. 2007;28 (14):2379–2384. doi:10.1002/elps.200600852
23. Zheng H, Li BH, Liu C, Jia L, Liu FT. Comprehensive analysis of lncRNA-mediated ceRNA crosstalk and identification of prognostic biomarkers in Wilms' tumor. *Biomed Res Int*. 2020;2020:4951692.
24. Jung DE, Park SB, Kim K, Kim C, Song SY. CG200745, an HDAC inhibitor, induces anti-tumour effects in cholangiocarcinoma cell lines via miRNAs targeting the Hippo pathway. *Sci Rep*. 2017;7 (1):10921. doi:10.1038/s41598-017-11094-3